Analytical and Bioanalytical Chemistry (2018) 410:5211–5218
https://doi.org/10.1007/s00216-018-1169-5

RESEARCH PAPER

Construction of a thermoresponsive magnetic porous polymer membrane enzyme reactor for glutaminase kinetics study

Liping Zhao[1,2] · Juan Qiao[1,3] · Meyong Hee Moon[4] · Li Qi[1,3]

Received: 3 April 2018 / Revised: 15 May 2018 / Accepted: 28 May 2018 / Published online: 16 June 2018

Abstract

Fabrication of polymer membranes with nanopores and a confinement effect toward enzyme immobilization has been an enabling endeavor. In the work reported here, an enzyme reactor based on a thermoresponsive magnetic porous block copolymer membrane was designed and constructed. Reversible addition–fragmentation chain transfer polymerization was used to synthesize the block copolymer, poly(maleic anhydride–styrene–*N*-isopropylacrylamide), with poly(*N*-isopropylacrylamide) as the thermoresponsive moiety. The self-assembly property of the block copolymer was used for preparation of magnetic porous thin film matrices with iron oxide nanoparticles. By covalent bonding of glutaminase onto the surface of the membrane matrices and changing the temperature to tune the nanopore size, we observed enhanced enzymolysis efficiency due to the confinement effect. The apparent Michaelis–Menten constant and the maximum rate of the enzyme reactor were determined (K_m = 32.3 mM, V_{max} = 33.3 mM min^{-1}) by a chiral ligand exchange capillary electrochromatography protocol with L-glutamine as the substrate. Compared with free glutaminase in solution, the proposed enzyme reactor exhibits higher enzymolysis efficiency, greater stability, and greater reusability. Furthermore, the enzyme reactor was applied for a glutaminase kinetics study. The tailored pore sizes and the thermoresponsive property of the block copolymer result in the designed porous membrane based enzyme reactor having great potential for high enzymolysis performance.

Keywords Porous block copolymer membrane · Enzyme kinetics study · Glutaminase · Chiral ligand exchange capillary electrochromatography

Introduction

Glutaminase (Glnase), a hydrolytic enzyme that catalyzes the conversion of L-glutamine (L-Gln) to L-glutamic acid, is widely used in biotechnology and clinical analysis [1–3]. In the medical field, Glnase has been used for enzymatic treatment of cancer, especially in acute lymphoblastic leukemia therapy [4]. Moreover, as an efficient antiretroviral agent, Glnase could also be used in the treatment of AIDS/HIV because it can decrease L-Gln levels in both serum and tissues for prolonged periods [5]. Importantly, the enzymatic activity and enzymolysis efficiency of Glnase would have a great influence on the diseases treatment [3]. Therefore, there is a growing de-

Liping Zhao and Juan Qiao contributed equally to this work.

Electronic supplementary material The online version of this article (https://doi.org/10.1007/s00216-018-1169-5) contains supplementary material, which is available to authorized users.

✉ Li Qi
qili@iccas.ac.cn

[1] Key Laboratory of Analytical Chemistry for Living Biosystems, Beijing National Laboratory for Molecular Sciences, Institute of Chemistry, Chinese Academy of Sciences, No. 2 Zhongguancun Beiyijie, Beijing 100190, China

[2] College of Chemistry & Environmental Science, Hebei University, Key Laboratory of Analytical Science and Technology of Hebei Province, Baoding 071002, China

[3] University of Chinese Academy of Sciences, No. 19A Yuquanlu, Beijing 100049, China

[4] Department of Chemistry, Yonsei University, 50 Yonsei-Ro, Seoul 03722, South Korea

mand for study of Glnase kinetics and determination of the enzymolysis efficiency of Glnase.

Usually, free Glnase in solution suffers from loss of stability, low enzymolysis efficiency, and poor reusability [6, 7]. Enzyme immobilization has been envisaged to enhance enzyme stability and preserve catalytic selectivity and enzymolysis efficiency even in harsh conditions, and allow the possibility of reuse. In general, immobilization occurs either on the surface of solid carriers (such as polymer- or silica-based nanoparticles) or through entrapping of the enzyme inside various porous materials (such as hydrogels, hollow fibers, and porous monoliths) [8–13]. A few studies focused on Glnase immobilization [14–17]. For example, Karahan et al. [15] modified Glnase on poly(acrylic acid) chains in the presence of Cu^{2+} ions. In the prepared enzyme reactor the stability of the immobilized Glnase was much greater than that of free Glnase in solution. Itoh et al. [17] used carbon-coated mesoporous silica as the material for trapping of Glnase and investigated the stability of the enzyme reactor at high pH. However, rare studies have been reported about the effects of changes in environmental conditions, especially temperature changes, on enzyme conformational changes, which may cause significant alteration of enzyme activity. Therefore, it is important and meaningful to use thermoresponsive block copolymers for immobilization of Glnase and for study of Glnase kinetics.

Among the various porous materials, porous polymer membranes that combine the properties of block copolymers and porous membranes have attracted attention with regard to enzyme immobilization because of their multiple functional sites, large surface area, and tunable pore sizes [18, 19]. In porous membranes, the small pores can accommodate the substrates and the enzymes in a small space, which can increase their collision opportunities through this confinement effect [20]. Consequently, the enzymolysis efficiency of the immobilized enzymes could be increased. Furthermore, block copolymers with multiple functional groups could provide sites for enzyme covalent immobilization. Importantly, block copolymers with stimuli-responsive moieties would provide a new strategy for tuning the pore sizes easily, which may further enhance the enzymolysis efficiency. Poly(*N*-isopropylacrylamide) (PNIPAm) is a thermoresponsive polymer that can curl to form micelle cavities when the temperature is higher than its lower critical solution temperature (LCST) [21]. Thus, it is speculated that the enzymolysis efficiency of Glnase should be increased with the combination of a porous membrane and micelle cavities of PNIPAm. However, there has been no report of a Glnase kinetics study based on the confinement effect of porous polymer membranes and the thermoresponsive property of block copolymers. On the other hand, in the catalytic process of Glnase, L-Gln is used as the enzyme substrate. To remove the interference of D-glutamine (D-Gln) in complex biosystems, a new method for chiral separation of D,L-amino acid enantiomers is needed.

In this work, the block copolymer poly(maleic anhydride–styrene–*N*-isopropylacrylamide), P(MAn-St-NIPAm), was synthesized by reversible addition–fragmentation chain transfer (RAFT) polymerization with PNIPAm as the thermoresponsive moiety. The ability to form a porous membrane and the ability of Glnase to covalently bond with the anhydride group of the poly(maleic anhydride–styrene), P(MAn-St), moiety in the block copolymer are demonstrated. The thermoresponsive enzyme reactor is combined with magnetic nanoparticles and displays the advantage of easy separation [22, 23]. Moreover, with use of L-Gln as the substrate, a Glnase kinetics study has been realized by chiral ligand exchange capillary electrochromatography (CLE-CEC). The enzymolysis efficiencies of free Glnase and P(MAn-St-NIPAm)-Glnase based thermoresponsive magnetic porous polymer membrane enzyme reactor (thermo-MPPMER) have been investigated. The proposed approach provides an appropriate system for testing porous block copolymer membranes as suitable matrices for use in enzyme kinetics studies.

Materials and methods

Reagents and materials

Styrene, maleic anhydride, L-arginine methyl ester dihydrochloride, and the initiator azobis(isobutyronitrile) were purchased from Shanghai Chemical Plant (Shanghai, China). Ferric chloride hexahydrate ($FeCl_3{\cdot}6H_2O$) and ferrous chloride tetrahydrate ($FeCl_2{\cdot}4H_2O$) for synthesis of magnetic Fe_3O_4 nanoparticles were obtained from Xilong Chemical Company (Guangdong, China). *N*-Isopropylacrylamide (NIPAM) and Coomassie brilliant blue G-250 were provided by Aladdin Reagent Co. (Shanghai, China). D,L-Amino acids, L-arginine, dansyl chloride, and the transfer agent benzyl benzodithioate were bought from Sigma-Aldrich (St Louis, USA). Glnase (from *Escherichia coli*) was obtained from Megazyme International Ireland (Bray, Ireland). Sodium hydroxide, ammonium hydroxide, zinc sulfate, tris(hydroxymethyl)aminomethane, lithium carbonate, $LiClO_4$, boric acid, sodium acetate, dimethyl sulfoxide, *N*,*N*-dimethylformamide, 1,4-dioxane, ethanol, tetrahydrofuran, chloroform, diethyl ether, and other reagents were provided by Beijing Chemical Corporation (Beijing, China). Milli-Q water (Millipore, Billerica, MA, USA) was used for the preparation of all the solutions.

Instruments

Chiral separation of dansyl-D,L-amino acids and the Glnase kinetics study were performed with a high-performance capillary electrophoresis analyzer (Beijing Institute of New

Technology and Application, Beijing, China). A 75-μm inner diameter × 60 cm (45-cm effective length) capillary (Yongnian Optical Fiber Factory, Hebei, China) was used for CLE-CEC experiments.

Polymer molecular weight was determined by gel permeation chromatography with a system composed of a Waters 1515 high-performance liquid chromatography pump, a Waters 2414 detector, and a set of Waters Styragel columns with *N*,*N*-dimethylformamide as the eluent at a flow rate of 1.0 mL/min.

A Bruker Tensor-27 spectrophotometer (wave number ranging from 4000 to 400 cm^{-1}) was used for characterization of the synthesized polymers by Fourier transform infrared (FT-IR) spectroscopy.

The morphologies of the bare capillary, coated capillary, and magnetic porous polymer membrane were obtained with a JSM-6510 scanning electron microscope (JEOL, Japan).

Thermogravimetric analysis was performed on a Pyris 1 thermogravimetric analyzer (PerkinElmer, Akron, OH) at a temperature ranging from 25 to 750 °C at a ramp rate of 20 °C/min.

Magnetic measurement was performed with a Lakeshore 7307 vibrating sample magnetometer at room temperature.

Fabrication of the thermo-MPPMER

Magnetic Fe_3O_4 nanoparticles were prepared according to [24]. First, 5.40 g (20.0 mM) $FeCl_3 \cdot 6H_2O$ and 1.98 g $FeCl_2 \cdot 4H_2O$ (10.0 mM) dissolved in 100.0 mL deionized water were put into a flask, then 25% ammonia was used to adjust the pH of the reactants to 12.0, and reaction occurred at 70 °C under stirring for 3 h. The magnetic Fe_3O_4 nanoparticles were obtained by washing of the products with deionized water and methanol until the pH was 7.0. Finally, the product was dried at 45 °C for 24 h. The size of the Fe_3O_4 nanoparticles was 63.4 ± 5.4 nm as measured by dynamic light scattering.

The macromolecular chain transfer agent P(MAn-St) was synthesized by RAFT polymerization; the process is described in detail in the electronic supplementary material. The thermoresponsive polymer, P(MAn-St-NIPAm), was also synthesized by RAFT polymerization. Briefly, NIPAm (300.0 mg), P(MAn-St) (300.0 mg), and the initiator azobis(isobutyronitrile) (10.0 mg) were dissolved in 10.0 mL tetrahydrofuran in a three-necked boiling flask. Then the reactant mixture was degassed by the freeze–pump–thaw method and reacted at 60 °C in an oil bath for 24 h. The reaction solution was poured into excess ester, and then the polymer products would precipitate. Finally, the obtained P(MAn-St-NIPAm) was filtered and dried at 45 °C for further use.

The thermoresponsive magnetic porous polymer membrane (thermo-MPPM) was fabricated by the breath figure method. Firstly, 30.0 mg P(MAn-St-NIPAm) was dissolved in 1.0 mL chloroform and mixed with 10.0 mg Fe_3O_4 nanoparticles. The porous membrane was prepared by dripping of the dissolved solution onto a glass pane, drop by drop, in a humid environment (relative humidity greater than 80%). The thermo-MPPM was obtained after the solvent had volatilized.

The size of Glnase was 73.4 ± 5.4 nm as measured by dynamic light scattering. The thermo-MPPMER was made by addition of 10.0 mg of the porous membrane and 1.0 mg $LiClO_4$ to 1.0 mL of 0.01 mg/mL enzyme solution (diluted with 5.0 mM sodium acetate, pH 4.9) followed by stirring for 3 h in an ice bath. The resultant thermo-MPPMER was washed with 5.0 mM sodium acetate (pH 4.9) three times before use. After use, the thermo-MPPMER was stored in sodium acetate buffer solution.

The amount of Glanse immobilized on the thermo-MPPMER was determined by the Bradford assay and calculated from the enzyme solution concentrations before and after immobilization. The detailed steps are described in the electronic supplementary material.

Kinetics study of the thermo-MPPMER

The kinetic constants of the thermo-MPPMER were determined by CLE-CEC. D,L-Glutamine (D,L-Gln) dissolved in the buffer solution (40.0 mM sodium acetate, adjusted to pH 4.9 with 36% acetic acid (v/v)) was used as the substrate of Glanse. The enzyme immobilization concentration and the chain length of the block copolymer were optimized for preparation of the enzyme reactor. The supernatant was collected by a magnet, derived with dansyl chloride, and then subjected to CLE-CEC determination. The kinetics study of the thermo-MPPMER was realized by addition of 200 μL L-Gln solution of various concentrations (0.9, 1.8, 3.0, 6.0, and 12.0 mM) to the enzyme reactor, followed by incubation for 1 min at 37 °C. The hydrolysis kinetic constants of free Glanse in solution and the enzyme reactor were calculated through the concentration change of L-Gln by the Michaelis–Menten constant (K_m) and the maximum rate (V_{max}). Three replicates were measured for each concentration.

Results

Construction and characterization of the thermo-MPPMER

P(MAn-St-NIPAm) was synthesized by RAFT polymerization; the synthesis process is displayed in Fig. S1. Then the resultant P(MAn-St-NIPAm) and the magnetic Fe_3O_4 nanoparticles were mixed and dissolved in chloroform. By use of the breath figure protocol, the solution was dropped onto a glass pane in a closed humidity environment (relatively humidity greater than 80%). Finally, the thermo-MPPM was

obtained after the solvent had evaporated totally (Fig. S2). There are various methods for enzyme immobilization on solid surfaces. Glnase was easily bound on the surface of the resultant thermo-MPPM through covalent bonding with the anhydride group. The thermo-MPPMER construction process is shown in Fig. S3.

FT-IR spectra proved the successful synthesis of the thermo-MPPM (Fig. S4). In the spectrum of Fe_3O_4, the typical peak of the Fe–O stretching vibration absorption was found at 590.2 cm^{-1}, and the absorption of –OH on the surface of the nanoparticles was observed at 3444.8 cm^{-1}. In the FT-IR spectra of the thermo-MPPM, other than the absorption peaks of Fe_3O_4 nanoparticles, the absorption peaks of C=C and CH_2 in the benzene ring were observed at 1454.3 and 2927.9 cm^{-1}, respectively. The stretching vibration absorption peaks of C=O in maleic anhydride were observed at 1778.3 and 1847.7 cm^{-1}. The stretching vibration absorption peak of O–H in amino amide at 1651.0 cm^{-1}, the bending vibration absorption peak of N–H at 1541.1 cm^{-1}, and stretching vibration absorption peaks of N–H at 3028.1 and 2927.9 cm^{-1} were also observed, which confirmed the successful synthesis of the thermo-MPPM.

A scanning electron microscopy image of the thermo-MPPM fabricated by the breath figure method is displayed in Fig. 1. The thermo-MPPM would offer anhydride bonds for Glnase immobilization through covalent bonding. Well-defined and uniform pores were observed, with pore sizes of less than 0.5 μm (Fig. 1a), and the thickness of the one-layer membrane was about 3.0 μm (Fig. 1b). Moreover, the nanospace and microspace provided by the pores could increase the collision opportunities of the immobilized Glnase and substrates, which would further enhance the hydrolysis efficiency.

Thermogravimetric analysis of Fe_3O_4 nanoparticles, the thermo-MPPM, and the thermo-MPPMER was used to identify the polymer membrane and the magnetic nanoparticles dispersed in the thermo-MPPM (Fig. S5). When the temperature was around 100 °C, a slight weight loss of the three samples was observed, which was caused by the loss of residual water. Then obvious weight loss of the thermo-MPPM and the thermo-MPPMER occurred at 400–500 °C, which was attributed to the degradation of the thermoresponsive polymer membrane and the immobilized enzyme. Moreover, the weight loss of the thermo-MPPMER was greater than that of the thermo-MPPM, which further verified the successful immobilization of Glnase.

Vibrating sample magnetometry was performed to investigate the magnetic properties of Fe_3O_4 nanoparticles, the thermo-MPPM, and the thermo-MPPMER. As shown in Fig. S6, the maximum saturation magnetization values of Fe_3O_4, the thermo-MPPM, and the thermo-MPPMER were 65.9, 12.4, and 11.9 emu/g, respectively. This revealed that the magnetization of Fe_3O_4 nanoparticles decreased when they were embedded in the thermo-MPPM and the thermo-MPPMER.

Thermoresponsive property of the enzyme reactor

Glnase was immobilized on the thermo-MPPM through covalent bonding with maleic anhydride groups in the block copolymer, and the influence of key factors on the Glnase hydrolysis efficiency was investigated. By use of the thermo-MPPMER as a biosensor for detection of L-Gln, the activity of the immobilized Glnase was evaluated by the percentage of substrate L-Gln hydrolyzed after incubation with the thermo-MPPMER, which was calculated by the following equation:

$$H(\%) = [(A_0 - A_{\text{L-Gln}})/A_0] \times 100\%, \quad (1)$$

where A_0 and $A_{\text{L-Gln}}$ are the peak areas of L-Gln before (Fig. 2a) and after thermo-MPPMER enzymolysis (Fig. 2b), respectively. The peak area was measured by the proposed CLE-CEC method as described in Figs. S7, S8, S9, S10, S11, S12, S13, S14, S15, and S16 and Tables S1, S2, and S3.

First, the influence of different mass ratios of P(MAn-St) to NIPAm on the hydrolysis efficiency was investigated. In the block copolymer synthesis process, the mass ratio of P(MAn-

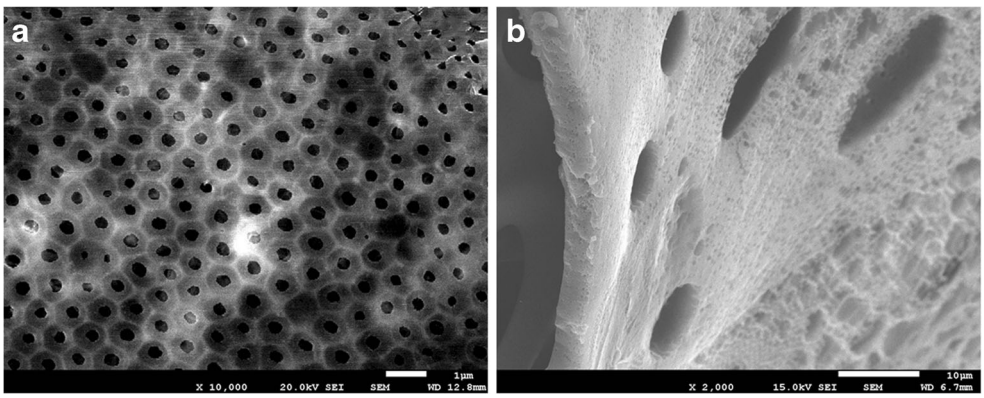

Fig. 1 Scanning electron microscopy images of the thermoresponsive magnetic porous polymer membrane fabricated with poly(maleic anhydride–styrene–*N*-isopropylacrylamide) at 30.0 mg/mL (the weight ratio of poly(maleic anhydride–styrene) to *N*-isopropylacrylamide was 1:1) and magnetic Fe_3O_4 nanoparticles at 10.0 mg/mL: **a** top surface and **b** cross section

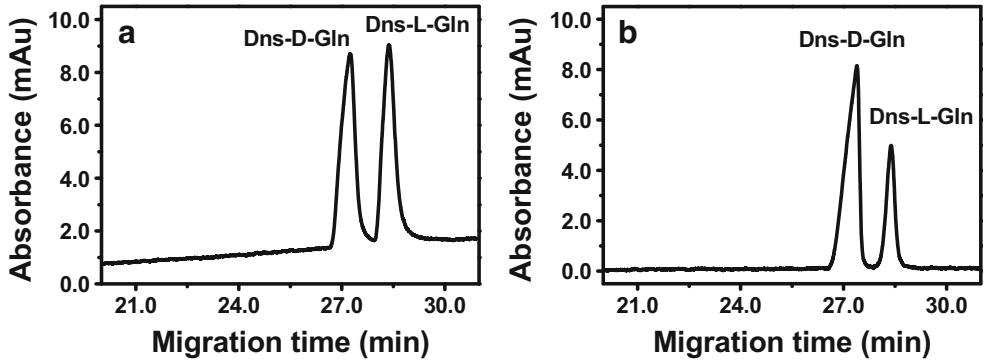

Fig. 2 Electrophoregrams of D, L-glutamine before (**a**) and after (**b**) glutaminase hydrolysis. The chiral ligand exchange capillary electrochromatography experimental conditions were as follows: buffer solution, 100.0 mM boric acid, 10.0 mM ammonium acetate, 4.0 mM Zn(II), and 4.0 mM L-arginine at pH 8.0; 1.0 mg thiourea at 1.0 mg/mL; applied voltage, -20 kV; sampling for 8 s in 15-cm height; detection wavelength, 254 nm; coated capillary, 75-μm inner diameter × 60 cm (45-cm effective length). D-Gln D-glutamine, Dns dansyl, L-Gln L-glutamine

St) to NIPAm was changed from 1.5:1 to 1:1.5. Three different mass ratio polymers were applied to fabricate the thermo-MPPMER. It was found that the mass ratio of NIPAm in the thermoresponsive block copolymer had an obvious influence on the hydrolysis efficiency (Fig. S17). When the ratio of P(MAn-St) to NIPAm was 1:1, the hydrolysis efficiency was greatest, so this ratio was selected for further studies.

In the Glnase immobilization process, the effect of different Glnase concentrations ranging from 0.005 to 0.015 mg/mL on the hydrolysis efficiency was investigated. Figure S18 indicates that the enzyme immobilization concentration had a significant influence on the hydrolysis efficiency. *H* increased greatly as the Glnase concentration increased from 0.005 to 0.01 mg/mL. A slight drop was observed when the Glnase concentration was increased to 0.015 mg/mL. Finally, 0.01 mg/mL as the best Glnase concentration was chosen for preparation of the thermo-MPPMER.

Next, at different temperatures, the thermoresponsive properties of the enzyme reactors were investigated. Figure 3 indicates that the thermo-MPPMER exhibited higher hydrolysis efficiency than free Glnase solution and the magnetic porous polymer membrane enzyme reactor, which demonstrated that the PNIPAm moiety in the thermo-MPPMER played an important role. The confinement effect of the porous block copolymer membrane increased the hydrolysis efficiency dramatically at 37 °C. In detail, the self-assembly property of the thermoresponsive block copolymer could tune the nanopore size by changing the hydrolysis temperature. It further led to enhancement of the enzymolysis efficiency because of the increased opportunities for collisions between the immobilized Glnase and the substrates.

Moreover, it is well known that the PNIPAm chain can curl to form micelle cavities when the temperature is higher than the LCST of PNIPAm. Once the hydrolysis temperature was 26 °C, the PNIPAm chains were likely extended (Fig. 4). When the hydrolysis temperature increased to 37 °C (LCST of PNIPAm), PNIPAm-based nano-sized micelle cavities could form (Fig. 4) and confined the immobilized Glnase and substrates in the smaller micellar space.

Further, the confinement effect of the nano-sized micelle cavities enhanced the probability of collision of the immobilized Glnase with the substrate. From Fig. 3 it can be observed that the hydrolysis efficiency of the thermo-MPPMER increased obviously when the temperature reached 37 °C in comparison with 26 °C, it, and then decreased at 60 °C. That might be because the PNIPAm-based nano-sized micelle cavities were destroyed at 60 °C (Fig. 4), which was higher than the LCST of PNIPAm. In addition, Glnase might be partially deactivated at a

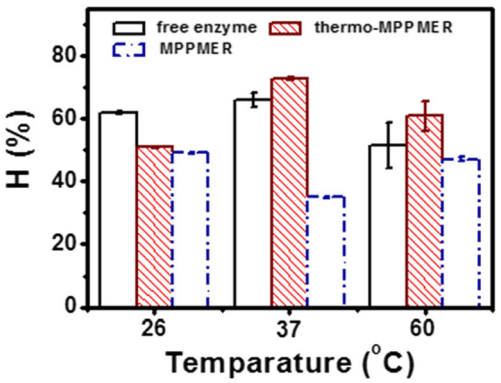

Fig. 3 Effect of temperature on the hydrolysis efficiency of free enzyme solution, the thermoresponsive magnetic porous polymer membrane enzyme reactor (thermo-MPPMER, P(MAn-St):NIPAm was 1:1), and the magnetic porous polymer membrane enzyme reactor (MPPMER, P(MAn-St):NIPAm was 1:0). The hydrolysis temperature was changed from 26 to 60 °C. The experimental conditions were as follows: free enzyme solution, 200 μL of 0.0087 mg/mL glutaminase solution incubated with 200 μL substrate; enzyme immobilization concentration, 0.01 mg/mL; immobilization time, 3 h

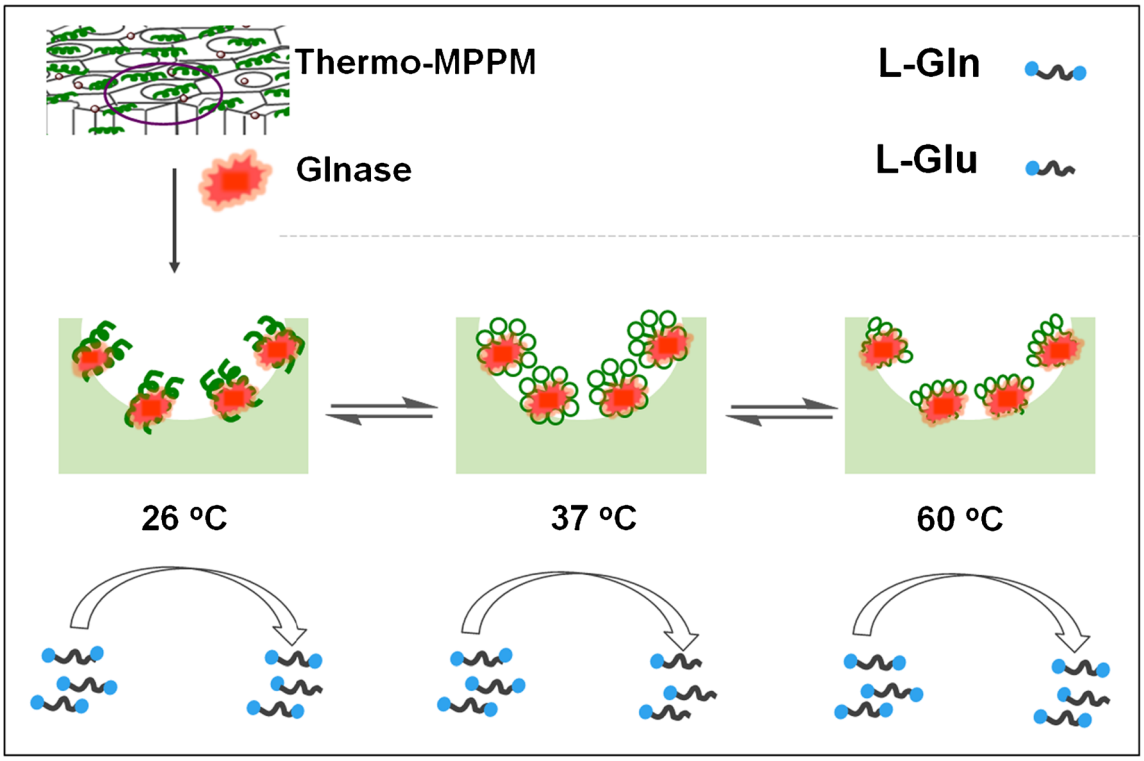

Fig. 4 Schematic illustration of the thermo-responsive property of the thermo-MPPMER for Glnase hydrolysis. L-Gln (L-glutamine) was the substrate of Glnase. L-Glu (L-glutamic acid) was the enzymatic reaction product

relatively high temperature. Therefore, hydrolysis at 37 °C was selected for the following investigation.

Finally, the amount of Glnase immobilized on the thermo-MPPMER was determined by the Bradford assay [25]. Different concentrations of enzyme solutions (0.001–0.2 mg/mL) were used to obtain the calibration curve (Fig. S19). The concentration of Glnase solutions before and after the immobilization was determined. By incubation with Coomassie brilliant blue solution for 2 min at 37 °C, the absorbance of Glnase solutions at 595 nm was detected. The results showed that 0.0087 mg Glanse per milliliter was immobilized on the enzyme reactor.

Glnase kinetics study of the thermo-MPPMER

Although D,L-Gln was used as the substrate of the thermo-MPPMER, its hydrolysis efficiency was calculated through the concentration change of L-Gln. To remove the interference of D-Gln in enzymatic hydrolysis in complicated living biosystems, it is necessary to perform chiral separation of D,L-Gln. CLE-CEC has been commonly used for chiral separation of amino acid enantiomers because of its high selectivity and high separation efficiency. In this study, a new CLE-CEC system was constructed and used for the Glnase kinetics study.

The kinetic constants of the enzyme reaction K_m and V_{max} were calculated by the Michaelis–Menten equation:

$$[S]/V = K_m/V_{max} + [S]/V_{max}, \quad (2)$$

where [S] is the concentration of the substrate, V is the enzyme reaction rate, K_m is the Michaelis–Menten constant, which represents the affinity of the enzyme, and V_{max} is the maximum enzymatic reaction velocity, which reflects the enzyme activity. K_m and V_{max} of the free Glnase solution were calculated as 6.8 mM and 6.7 mM/min, respectively. The Lineweaver–Burk plot of Glnase in free enzyme solution is shown in Fig. S20.

Figure 5 displays the Lineweaver–Burk plot of the immobilized Glnase; the linear relationship was $y = 0.967x + 0.031$ ($R^2 = 0.995$). The K_m and V_{max} values of the thermo-

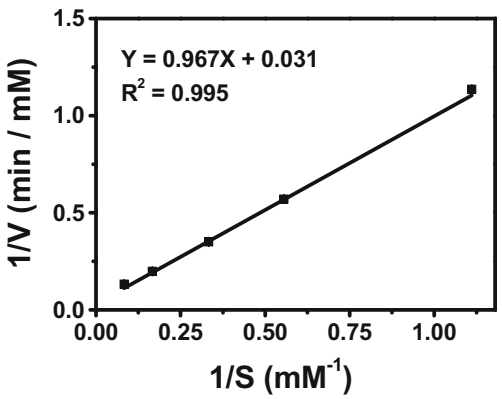

Fig. 5 Lineweaver–Burk plot of the thermoresponsive magnetic porous polymer membrane enzyme reactor

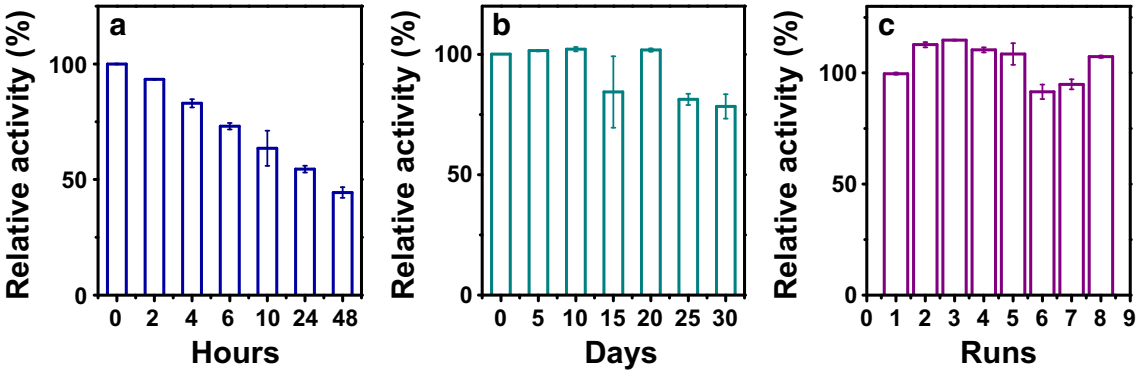

Fig. 6 Stability of free glutaminase in solution (**a**), and stability (**b**) and reusability (**c**) of the thermoresponsive magnetic porous polymer membrane enzyme reactor

MPPMER calculated from the Lineweaver–Burk plot were 32.3 mM and 33.3 mM/min, respectively. Compared with K_m of the free enzyme solution, K_m of the thermo-MPPMER was much higher, which might be because the enzyme immobilization decreased the chance of the substrate contacting with the enzyme active sites. The ability of the immobilized enzyme to bind to the substrate was decreased. V_{max} of the thermo-MPPMER was four times higher than that of the free enzyme solution. The data indicated a higher hydrolysis rate of the thermo-MPPMER compared with the free enzyme solution owing to the confinement effect of the porous membrane material. Furthermore, the thermoresponsive property of PNIPAm strengthened the confinement effect, which induced a much higher hydrolysis efficiency.

The reusability and stability of the thermo-MPPMER were also investigated. Because of the magnetic property of the enzyme reactor, the substrate could be easily separated from the thermo-MPPMER matrix. Figure 6a shows that after 48 h the relative activity of free Glnase dropped to 44.3%, whereas the relative activity of the thermo-MPPMER was 78.3% after 30 days of storage (Fig. 6b), which indicated good stability of the proposed enzyme reactor. Moreover, the reusability of the thermo-MPPMER was studied. The results revealed that the thermo-MPPER could endure eight consecutive uses (Fig. 6c), which indicated good reusability of the prepared enzyme reactor.

Conclusions

An efficient immobilization strategy requires a rational selection of supporting materials and of the binding protocol to achieve fine control over the conformation and spatial and orientational arrangement of the enzyme on the support. In this study, a simple approach for fabrication of a P(MAn-St-NIPAm)-based membrane that could act as the support for covalent bonding of Glnase was designed and reported. The prepared thermo-MPPMER was successfully used for a Glnase kinetics study. On the basis of the merits of the thermoresponsive property of the PNIPAm moiety in P(MAn-St-NIPAm) and the confinement effect of the porous block copolymer membrane, the enzyme reactor has demonstrated its good performance in enhancing the enzymolysis efficiency in comparison with free Glnase. The proposed cost-effective enzyme reactor also displayed good stability and reusability. Moreover, our approach for construction of more polymer-based enzyme reactors means that the thermoresponsive property of P(MAn-St-NIPAm) has great potential in enzyme kinetics studies.

Acknowledgements This study was financially supported by the National Natural Science Foundation of China (grants 21575144, 21475137, 21611540335, 21727809, 21635008, and 21621062) and the Chinese Academy of Sciences (QYZDJ-SSW-SLH034). MHM is appreciative of support from the National Research Foundation of Korea (NRF-016K2A9A2A06004726).

Compliance with ethical standards

Conflict of interest The authors declare that they have no competing interests.

References

1. Nanga RPR, DeBrosse C, Singh A, D'Aquilla K, Hariharan H, Reddy R. Glutaminase catalyzes reaction of glutamate to GABA. Biochem Biophys Res Commun. 2014;448(4):361–4.
2. Yano S, Kamemura A, Yoshimune K, Moriguchi M, Yamamoto S, Tachiki T, et al. Analysis of essential amino acid residues for catalytic activity of glutaminase from micrococcus luteus K-3. J Biosci Bioeng. 2006;102(4):362–4.
3. Sido B, Seel C, Hochlehnert A, Breitkreutz R, Dröge W. Low intestinal glutamine level and low glutaminase activity in Crohn's disease: a rational for glutamine supplementation? Dig Dis Sci. 2006;51(12):2170–9.
4. Sarada KV. Production and applications of L-glutaminase using fermentation technology. Asia Pac J Res. 2013;1:1–4.
5. Binod P, Sindhu R, Madhavan A, Abraham A, Mathew AK, Beevi US, et al. Recent developments in L-glutaminase production and applications – an overview. Bioresour Technol. 2017;245:1766–74.

6. Wang H, Jiao F, Gao F, Zhao X, Zhao Y, Shen Y, et al. Covalent organic framework-coated magnetic graphene as a novel support for trypsin immobilization. Anal Bioanal Chem. 2017;09(8):2179–87.
7. Sirisha VL, Jain A. Enzyme immobilization: an overview on methods, support material, and applications of immobilized enzymes. Adv Food Nutr Res. 2016;79:179–211.
8. Guo C, Zhao X, Zhang W, Bai H, Qin W, Song H, et al. Preparation of polymer brushes grafted graphene oxide by atom transfer radical polymerization as a new support for trypsin immobilization and efficient proteome digestion. Anal Bioanal Chem. 2017;409(20):4741–9.
9. Wan Y, Zhao D. On the controllable soft-templating approach to mesoporous silicates. Chem Rev. 2007;107(7):2821–60.
10. Bergman J, Wang Y, Wigström J, Cans AS. Counting the number of enzymes immobilized onto a nanoparticle-coated electrode. Anal Bioanal Chem. 2018;410(6):1775–83.
11. Kalogeris E, Sanakis Y, Mamma D, Christakopoulos P, Kekos D, Stamatis H. Properties of catechol 1.2-dioxygenase from Pseudomonas putida immobilized in calcium alginate hydrogels. Enzym Microb Technol. 2006;39(5):1113–21.
12. Liu X, Wong DKY. Electrocatalytic detection of estradiol at a carbon nanotube|Ni(cyclam) composite electrode fabricated based on a two-factorial design. Anal Chim Acta. 2007;594(2):184–91.
13. Ponomareva EA, Volokitina MV, Vinokhodov DO, Vlakh EG, Tennikova TB. Biocatalytic reactors based on ribonuclease A immobilized on macroporous monolithic supports. Anal Bioanal Chem. 2013;405(7):2195–206.
14. Shigeki K, Makoto H, Tetsuya Y. Preparation of magnetic support for glutaminase immobilization. Nippon Shokuhin Kogyo Gakkaishi. 1994;41(1):31–6.
15. Karahan M, Karakuş E, Bülbül D, Atacı N. Immobilization of glutaminase enzyme from Hypocria jecorina on polyacrylic acid: preparation and biochemical characterization. Artif Cells Nanomed Biotechnol. 2014;42(4):262–7.
16. Moser I, Jobst G, Aschauer E, Svasek P, Varahram M, Urban G. Miniaturized thin film glutamate and glutamine biosensors. Biosens Bioelectron. 1995;10(6-7):527–32.
17. Itoh T, Hoshikawa Y, Matsuura SI, Mizuguchi J, Arafune H, Hanaoka TA, et al. Production of L-theanine using glutaminase encapsulated in carbon-coated mesoporous silica with high pH stability. Biochem Eng J. 2012;68:207–14.
18. Jiang JF, Qiao J, Mu XY, Moon MH, Qi L. Fabrication of enzyme reactor utilizing magnetic porous polymer membrane for screening D-amino acid oxidase inhibitors. Talanta. 2017;165:251–7.
19. Feng WY, Qiao J, Jiang JF, Sun B, Li Z, Qi L. Development of alanine aminotransferase reactor based on polymer@Fe_3O_4 nanoparticles for enzyme inhibitors screening by chiral ligand exchange capillary electrophoresis. Talanta. 2018;182:600–5.
20. Chen ZJ, Guan ZH, Li MR, Yang QH, Li C. Enhancement of the performance of a platinum nanocatalyst confined within carbon nanotubes for asymmetric hydrogenation. Angew Chem Int Ed. 2011;50(21):4913–7.
21. Yang JS, Qiao J, Kim JY, Zhao LP, Qi L, Moon MH. Online proteolysis and glycopeptide enrichment with thermoresponsive porous polymer membrane reactors for nanoflow liquid chromatography-tandem mass spectrometry. Anal Chem. 2018;90:3124–31.
22. Huber DL. Synthesis, properties, and applications of iron nanoparticles. Small. 2005;1(5):482–501.
23. Niu M, Pham-Huy C, He H. Core-shell nanoparticles coated with molecularly imprinted polymers: a review. Microchim Acta. 2016;183(10):2677–95.
24. Mu XY, Qiao J, Qi L, Dong P, Ma HH. Poly(2-vinyl-4,4-dimethylazlactone)-functionalized magnetic nanoparticles as carriers for enzyme immobilization and its application. ACS Appl Mater Interfaces. 2014;6(23):21346–54.
25. Ma JF, Liang Z, Qiao XQ, Deng QL, Tao DY, Zhang LH, et al. Organic-inorganic hybrid silica monolith based immobilized trypsin reactor with high enzymatic activity. Anal Chem. 2008;80(8):2949–56.